

Functionalized Pentacene: Improved Electronic Properties from Control of Solid-State Order

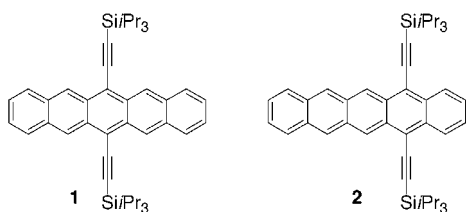
John E. Anthony,^{*,†} James S. Brooks,[‡] David L. Eaton,[†] and Sean R. Parkin[†]

Department of Chemistry, University of Kentucky
Lexington, Kentucky 40506-0055
FSU/NHMFL, 1800 East Paul Dirac Drive
Florida State University, Tallahassee Florida 32310

Received May 22, 2001

Molecular order has proven to be a significant factor in the performance of devices based on organic semiconductors. Recent studies involving solubilized versus unsubstituted thiophene oligomers have demonstrated that modifications which increase orbital overlap in the solid state can improve device performance by more than an order of magnitude.¹ Similar studies on pentacene, a compound which has already demonstrated remarkable potential for device applications,² have also focused on maximizing orbital overlap by inducing order in films.³ However, these pentacene studies have thus far relied on substrate modification, rather than on pentacene functionalization,⁴ to achieve the desired goals. We report here the preparation of two *functionalized* pentacene derivatives, and the effect of this functionalization on both the solid-state ordering and the electronic properties of the resulting crystals.

Our goal for a functionalized pentacene was two-fold: First, the substituents should impart solubility to the acene, to simplify purification and processing. Second, the substituents should induce some capability for self-assembly of the aromatic moieties into π -stacked arrays to enhance intermolecular orbital overlap. We anticipated that both of these goals could be accomplished by exploiting a rigid spacer to hold the necessarily bulky solubilizing groups well away from the aromatic core, allowing the closest possible contact between the aromatic rings.⁵ Our initial targets were the bis(triisopropylsilyl)ethynyl)pentacenes **1** and **2**. Both of these compounds are easily prepared in near quantitative yield in a one-pot reaction from 6,13-pentacenequinone and 5,14-pentacenequinone, respectively.⁶



[†] University of Kentucky

[‡] Florida State University, FSU/NHMFL

(1) (a) Dodabalapur, A.; Torsi, L.; Katz, H. E. *Science* **1995**, *268*, 270. (b) Horowitz, G.; Fichou, D.; Peng, X.; Xu, Z.; Garnier, F. *Solid State Commun.* **1989**, *72*, 381. (c) Garnier, F.; Hajlaoui, R.; Yassar, A.; Srivastava, P. *Science* **1994**, *265*, 1684. (d) Garnier, F.; Horowitz, G.; Fichou, D.; Yassar, D. *Synth. Met.* **1996**, *81*, 163. (e) Dimitrakopoulos, C. D.; Furman, B. K.; Graham, T.; Hegde, S.; Purushothaman, S. *Synth. Met.* **1998**, *92*, 47.

(2) (a) Schön, J. H.; Kloc, Ch.; Batlogg, B. *Science* **2000**, *288*, 2338. (b) Schön, J. H.; Berg, S.; Kloc, Ch.; Batlogg, B. *Science* **2000**, *287*, 1022. (c) Schön, J. H.; Kloc, Ch.; Batlogg, B. *Science* **2000**, *406*, 702. (d) Schön, J. H.; Kloc, Ch.; Bucher, E.; Batlogg, B. *Synth. Met.* **2000**, *115*, 177. (e) Dimitrakopoulos, C. D.; Purushothaman, S.; Kymissis, J.; Callegari, A.; Shaw, J. M. *Science* **1999**, *283*, 822. (f) Dimitrakopoulos, C. D.; Kymissis, J.; Purushothaman, S.; Neumayer, D. A.; Duncombe, P. R.; Laibowitz, R. B. *Adv. Mater.* **1999**, *11*, 1372.

(3) Lin, Y. Y.; Gundlach, D. J.; Nelson, S.; Jackson, T. N. *IEEE Trans. Electron Devices* **1997**, *44*, 1325.

(4) For results using spin-cast films of pentacene with *removable* solubilizing groups: Herwig, P. T.; Müllen, K. *Adv. Mater.* **1999**, *11*, 480.

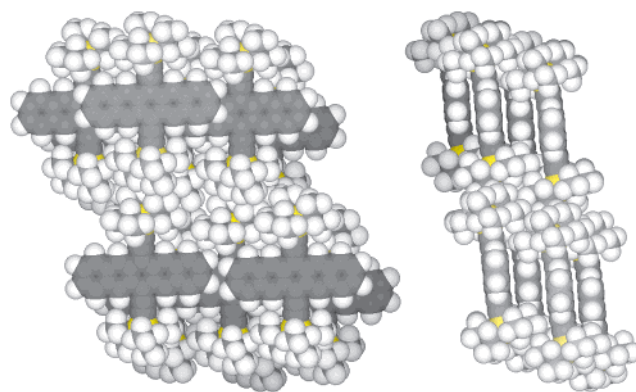


Figure 1. Solid-state ordering of **1**. (Left) View of the *ac* layer (looking down the *b* axis). (Right) View of the *bc* layer (looking down the *a* axis).

Pentacene **1** is very soluble in most organic solvents. Relatively large crystals (plates, 1 mm \times 1 mm \times 0.1 mm) were easily grown from acetone and analyzed by X-ray diffraction.⁷

Comparison of the solid-state ordering of substituted pentacene **1** with that of unsubstituted pentacene reveals striking differences (Figure 1). Most apparently, **1** does not adopt the herringbone pattern of unsubstituted pentacene. Rather, it stacks in a two-dimensional columnar array with significant overlap of the pentacene rings in adjacent molecules. Because of this arrangement, the interplanar spacing of the aromatic rings is significantly smaller in the substituted system (3.47 Å for **1**, compared with 6.27 Å for unsubstituted pentacene⁸).

The unique arrangement of molecules in the solid state should lead to significant anisotropy of resistivity in the crystal. To determine the magnitude of this effect we performed a series of 4-terminal resistivity measurements on several different crystals of **1**, with leads in the “Montgomery method” configuration.⁹ Resistivity measured along the *b* axis, perpendicular to the plane of the pentacene rings, was the lowest ($2.5 \times 10^6 \Omega\text{-cm}$), followed closely by that measured parallel to the long axis of the molecules (the *a* axis, $5 \times 10^8 \Omega\text{-cm}$). The resistivity across the short (*c*) axis is particularly high ($3 \times 10^{10} \Omega\text{-cm}$) due to the insulating barrier created by the solubilizing groups. All of these values are significantly lower than those reported for high-purity pentacene crystals ($10^{12} \Omega\text{-cm}$).¹⁰

We prepared asymmetric derivative **2** because we envisioned that a near-perfect stacking of this compound could be possible in the solid state. Crystallographic analysis¹¹ of this material (Figure 2) supported at least part of this hypothesis: The molecule does form nearly perfect stacked pairs, with the solubilizing groups arranged to minimize steric interactions. Unfortunately, these pairs then pack in a herringbone pattern similar to that observed for unsubstituted pentacene. As expected, this solid-

(5) Anthony, J.; Boldi, A. M.; Boudon, C.; Gisselbrecht, J.-P.; Gross, M.; Seiler, P.; Knobler, C. B.; Diederich, F. *Helv. Chim. Acta* **1995**, *78*, 797.

(6) The purity and structure of all new compounds were confirmed by ¹H and ¹³C NMR, IR, UV, MS, and EA. Synthetic details are provided as Supporting Information.

(7) X-ray data for **1**; triclinic space group $P\bar{1}$, $D_c = 1.104 \text{ g cm}^{-3}$, $Z = 1$, $a = 7.5650(15) \text{ \AA}$, $b = 7.7500(15) \text{ \AA}$, $c = 16.835(3) \text{ \AA}$, $\alpha = 89.15(3)^\circ$, $\beta = 92.713(10)^\circ$, $\gamma = 83.63(3)^\circ$, $V = 960.9(3) \text{ \AA}^3$. Final $R(F) = 0.0486$, $wR_2(F^2) = 0.1039$ for 232 variables and 3375 data. Details provided as Supporting Information.

(8) Cornil, J.; Calbert, J. Ph.; Brédas, J. L. *J. Am. Chem. Soc.* **2001**, *123*, 1250.

(9) Montgomery, H. C. *J. Appl. Phys.* **1971**, *42*, 2971.

(10) Schön, J. H.; Kloc, Ch.; Batlogg, B. *Appl. Phys. Lett.* **2000**, *77*, 2473.

(11) X-ray data for **2**; monoclinic space group $C2/c$, $D_c = 1.094 \text{ g cm}^{-3}$, $Z = 8$, $a = 28.222(3) \text{ \AA}$, $b = 18.904(2) \text{ \AA}$, $c = 14.555(2) \text{ \AA}$, $\beta = 92.713(10)^\circ$, $V = 7756.5(16) \text{ \AA}^3$. Final $R(F) = 0.0568$, $wR_2(F^2) = 0.1080$ for 471 variables and 6843 data. Details provided as Supporting Information.

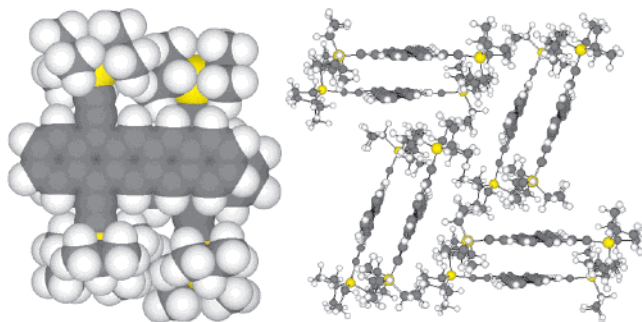


Figure 2. View of the close-packing "dimeric" stacks of **2** (left) and their arrangement in the solid state (right).

state arrangement leads to very high resistivity along all crystallographic axes. The lowest resistivity measured for this material was $8 \times 10^9 \Omega\text{-cm}$. This value still compares quite favorably with that of unsubstituted pentacene and is even lower than the resistivity of **1** along its least-conductive axis.

An additional demonstration of the remarkably low resistivity associated with crystalline **1** can be seen in the Arrhenius plot of resistivity versus inverse temperature for **1** and **2** (Figure 3). Measurement of resistivity in these samples was complicated by apparent capacitive charging of the material at low temperatures, so that the temperature-dependent resistivity was most easily acquired by first heating the sample and monitoring the resistivity as the sample cooled. The data thus acquired was used to derive the band gap along the three crystallographic axes of **1**, as well as the band gap for **2**. As expected, the band gaps mirror the resistivity data. The gap measured down the π -stacking axis of **1** was the smallest (0.6 eV),¹² and that measured across the channels of solubilizing groups (the *c* axis, Figure 1) was the largest (0.9 eV). The offset pentacene **2** yielded a band gap of 1.83 eV—essentially identical to the absorption edge found in the optical spectrum (~ 660 nm for a thin film).

More technologically relevant is the resistivity of thin films of these materials, which were easily prepared by either spin-casting or vacuum evaporation. While films of **1** proved to be quite robust, films of **2** decomposed rapidly upon exposure to air. The sheet resistivity of solvent-cast films of **1** is approximately $10^{10} \Omega/\text{square}$. Vacuum-evaporated films of **1** had significantly improved electronic properties, with surface resistivities on the order of $10^8 \Omega/\text{square}$. For a 5000 Å thick film, this value translates to a resistivity of $\sim 10^6 \Omega\text{-cm}$ —the same order of magnitude as the resistivity along the π -stacking axis of crystalline **1**—implying the formation of a highly ordered film. X-ray diffraction analysis of this film gave rise to sharp diffraction peaks showing a layer separation of 16.83 Å, identical to the *c*-axis

(12) Confirmed by examination of the NIR spectrum of powdered **1**, which showed a strong absorption at 4380 cm^{-1} (0.56 eV).

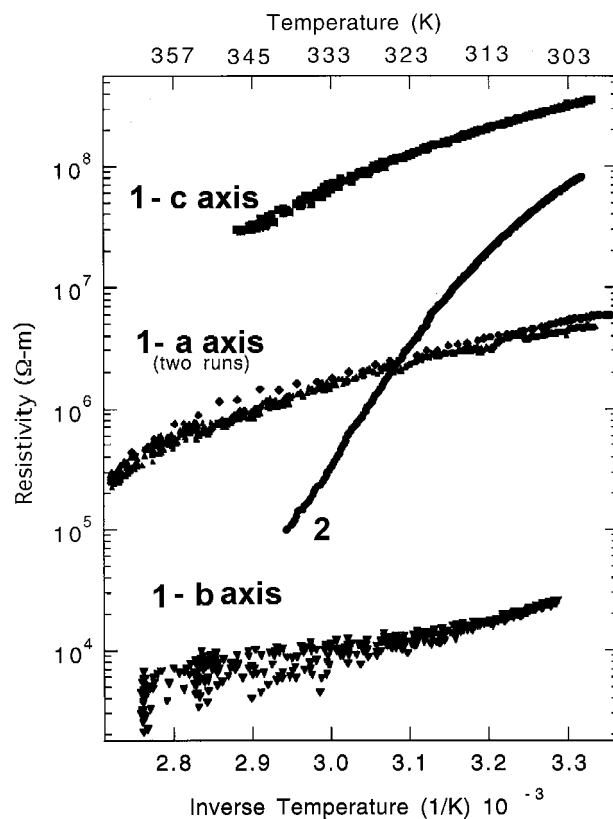


Figure 3. Plot of resistivity vs temperature along all three crystallographic axes of **1**, and along one axis of **2**.

unit cell length. Thus, the films grow with the silyl groups on the surface of the glass, leading to π -stacking in the direction of current flow.

With these two selectively functionalized pentacene derivatives, we have demonstrated significant conductivity enhancements by controlling the arrangement of the molecules in the solid state. This example demonstrates that simultaneous improvement in ease of processing and in electronic properties is achievable.

Acknowledgment. J.E.A. thanks the Office of Naval Research (N00014-99-1-0859) and the National Science Foundation (CAREER Award CHE-9875123) for generous support of this research. We thank Professor Carolyn Brock for helpful discussions and Mr. Matt Krepps for performing combustion analysis on **1** and **2**.

Supporting Information Available: Synthetic procedures, characterization (PDF) and X-ray crystallographic data (CIF) for compounds **1** and **2**. This material is available free of charge via the Internet at <http://pubs.acs.org>.

JA0162459